Rare earth element distribution in the NE Atlantic

Evidence for the temporal and spatial stability of the seawater signature and the influence of benthic sources

Kirsty Crocket[1] k.crocket@ed.ac.uk, Emily Hill[2], Richard E. Abell[2], Clare Johnson[2], Stefan E. Gary[2], Tim Brand[2], Ed C. Hathorne[3]
[1]University of Edinburgh, UK, [2]SAMS, UK, [3]GEOMAR, Germany

Funded by SAMS, NERC National Capability Funding for the Extended Ellett Line, MASTS, and H2020 ATLAS project.

EEL Hydrography & REE concentrations

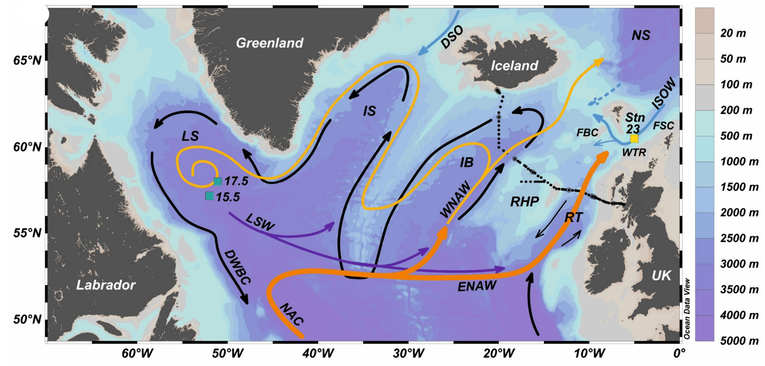

Fig. 1 ↑ Location map with 2015 EEL stations (black dots), deep ocean currents (black), cold overflow currents (blue), surface currents (orange and yellow). Faroe-Shetland Channel (FSC), Faroe Bank Channel (FBC), Wyville Thomson Ridge (WTR). Station 23 (Lacan and Jeandel, 2004), Stations 17.5 and 15.5 (Filippova et al., 2017).
Water masses: Deep Western Boundary Current (DWBC), Labrador Sea Water (LSW), Iceland-Scotland Overflow Water (ISOW), Denmark Strait Overflow (DSO), North Atlantic Current (NAC), Western North Atlantic Water (WNAW), Eastern North Atlantic Water (ENAW). ***Ocean basins:*** Labrador Sea (LS), Iceland Basin (IB), Irminger Sea (IS), Rockall-Hatton Plateau (RHP), Rockall Trough (RT), Norwegian Sea (NS). Figure created using ODV software, available at https://odv.awi.de/ (Schlitzer, 2016).

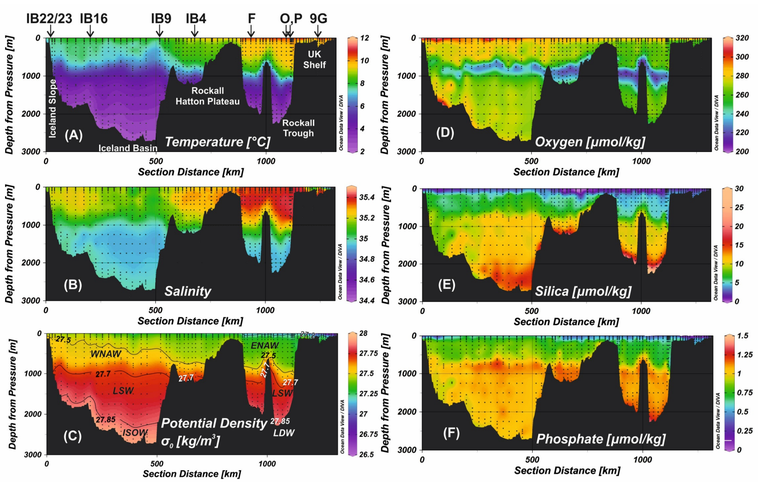

Fig. 2 ↑ Sections of (A) potential temperature (°C), (B) salinity, (C) potential density σθ (kg/m³), (D) dissolved oxygen (µmol/kg), (E) silica (µmol/kg), (F) phosphate (µmol/kg). The potential density section has contours delineating the ranges identified by Holliday et al. (2015) as representative of different water masses. The data are from 920 bottle samples (black dots) collected from 85 stations over ~1300 km of cruise track. Figure created using ODV software (Schlitzer, 2016).

Seawater rare earth element (REE) concentrations are increasingly applied to reconstruct water mass histories by exploiting relative changes in the normalised patterns.

However, the mechanisms by which water masses gain their REE patterns are not fully understood.

We collected water samples at 8 stations on the EEL (Figs 1-3), and measured dissolved REE by offline automated chromatography (SeaFAST) + ICP-MS.

The proximity to two continental boundaries, the incipient spring bloom at the time of the cruise, and the importance of deep water circulation in this climatically sensitive gateway region make it an ideal location to investigate sources of REE to seawater and the effects of vertical cycling and lateral advection on their distribution.

Temporal REE stability

IB16 (1500 m) and deep IB9 show pISOW-normalised values close to unity, and suggest ISOW REE composition is stable on at least decadal timescales.

Absence of overlap at IB4 indicates that ISOW does not circulate on Rockall-Hatton Plateau.

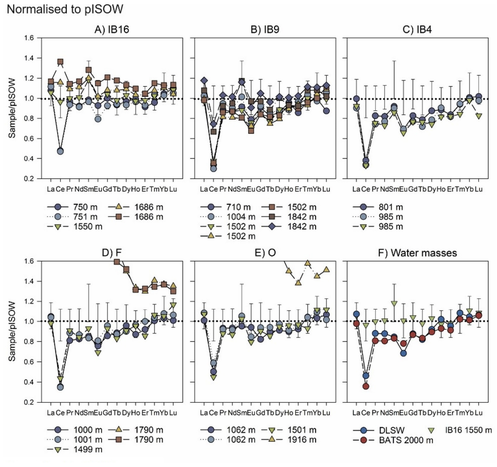

Fig. 7 (i) ↙ (A-E) Normalisation by pISOW of the REE data at the 5 open ocean stations on the EEL. (F) Normalisation by pISOW of DLSW and BATS 2000 m. Error bars represent the combined 2SD from normalisation of IB16 (1550 m) by pISOW. REE concentrations for BATS (van de Fliert et al., 2012), pISOW (Lacan and Jeandel, 2004), and DLSW (Filippova et al., 2017).

Fig. 7 (ii) ↘ (G-K) Normalisation by deep (D)LSW of the REE data at the 5 open ocean stations on the EEL. (L) Normalisation by DLSW of pISOW and BATS 2000 m. Error bars represent the combined 2SD from normalisation of IB16 (1550 m) by pISOW. REE concentrations for BATS (van de Fliert et al., 2012), pISOW (Lacan and Jeandel, 2004), and DLSW (Filippova et al., 2017). The symbols used above are the same as in Fig. 7(i).

Spatial REE stability

Values close to unity are observed at F, O (excluding deepest samples) and IB4, indicating the predominance of LSW at the these stations (Fig. 7(ii)).

ISOW and LSW are most clearly differentiated by LREE and MREE concentrations. They are ~15% lower in LSW relative to ISOW, with prominent depletions of ~50% Ce and ~30% Eu.

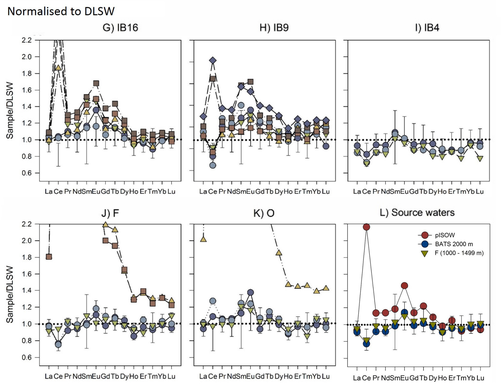

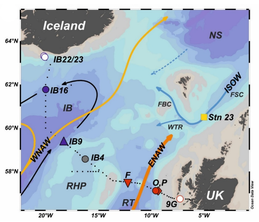

Fig. 3 ↑ Detailed view of the 2015 EEL stations, with those sampled in this study highlighted by large labelled symbols (blue, red, grey). Figure created using ODV software (Schlitzer, 2016).

Benthic flux

~10% pore water contribution in the deep Rockall Trough and ≤25% in coastal waters. Negligible contributions to other parts of the water column.

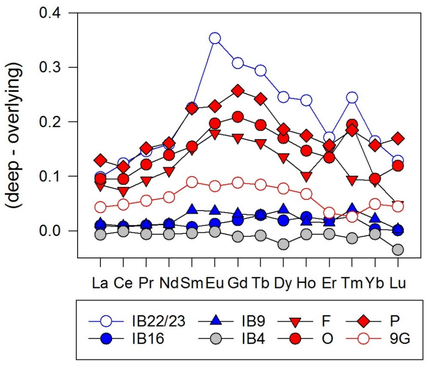

Fig. 8 ↗ "Excess" REE_N (PAAS normalised) in the deepest seawater samples from each open ocean station to identify the phase contributing excess REE concentrations to the water column, calculated by subtracting the PAAS-normalised REE in the overlying sample from the deepest sample at each of the EEL stations (REE_N deepest sample – REE_N overlying sample).

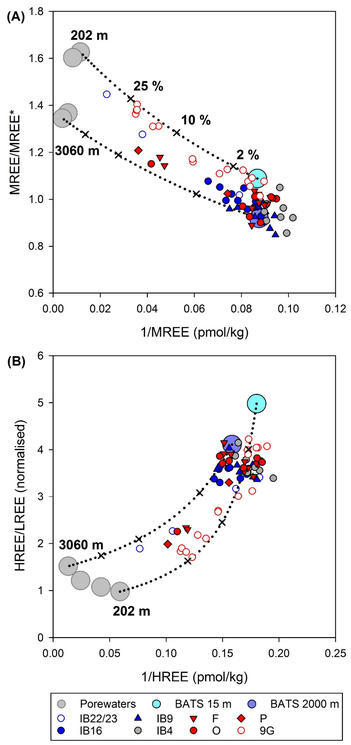

Fig. 9 ← Mixing plots of (A) MREE/MREE* vs. 1/MREE, and (B) HREE/LREE vs. 1/HREE, to highlight the combined effects of REE composition and concentration. The MREE/MREE* and HREE/LREE are calculated using PAAS-normalised data, vs. the non-normalised concentrations for 1/MREE and 1/HREE (pmol/kg). Mixing lines (black dotted lines) and mixing proportions (black crosses). BATS seawater 15 m and 2000 m (van de Fliert et al., 2012), pore waters (Abbott et al., 2015).

Biogeochemical cycling

Similarity in ODZ-surface REE difference to bacteria/water REE partitioning (Fig. 10) suggests causal link.

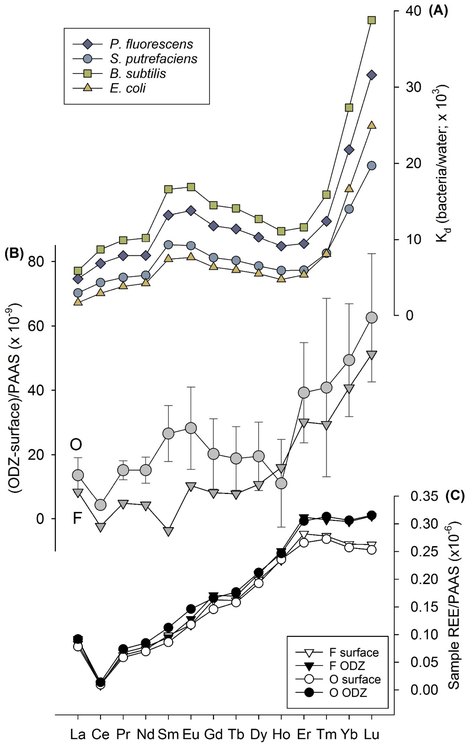

Fig. 10 → Comparison of (A) the REE partitioning behaviour from water to bacteria, with (B) the PAAS-normalised difference between the oxygen depletion zone (ODZ) and surface REE concentrations. For clarity, the 1SD propagated errors are shown for O only. (C) The PAAS-normalised distribution profiles of F and O showing only the surface and oxygen depletion zone data to highlight the lower REE concentrations in the surface waters. The REE partitioning data in (A) are from Takahashi et al. (2006, 2007), from experiments at pH 4 and I=0.01 M NaCl.

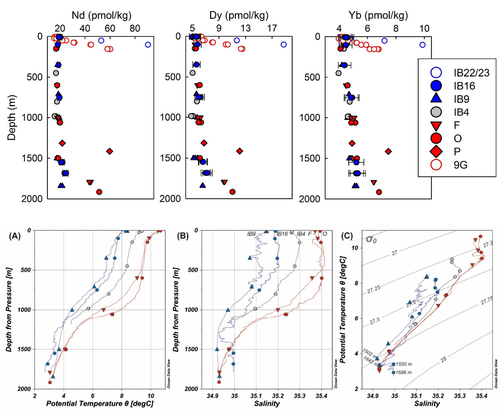

Fig. 4 ← Concentration-depth profiles of selected REE to span the light (Nd), middle (Dy) and heavy (Yb) range. Concentrations are in pmol/kg. Error bars represent 2σ uncertainty from repeat measurement of BATS 2000 m reference seawater. To note, surface samples from O and all 9G were not filtered.

Fig. 5 ← (A) Depth (m) vs. potential temperature (°C), (B) depth vs. salinity, (C) potential temperature vs. salinity with grey isopycnals lines, for open ocean stations. Sample data are indicated by symbols that correspond to those on Fig. 2. Deepest samples at IB16 are labelled. Figure created using ODV software (Schlitzer, 2016).

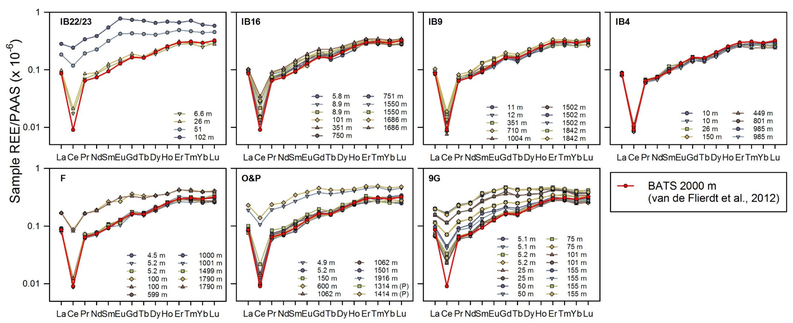

Fig. 6 ↑ REE data normalised to the Post-Archaean Shale (PAAS) value as reported in Freslon et al., (2014). The BATS 2000 m pattern (van de Fliert et al., 2012) is shown for comparison (bold red line). To note, surface samples from O and all 9G were not filtered.